Josephson supercurrent in a graphene-superconductor junction

E. Sarvestani[1] and S. A. Jafari[2,3]

[1]*Department of Physics, Isfahan University of Technology, Isfahan 84156-83111, Iran*

[2]*Department of Physics, Sharif University of Technology, Tehran 11155-9161, Iran*

[3]*School of Physics, Institute for Research in Fundamental Sciences (IPM), Tehran 19395-5531, Iran*

(Received 28 July 2011; revised manuscript received 13 October 2011; published 6 January 2012)

Within the tunneling Hamiltonian formulation for the eight-component spinors, the Josephson critical supercurrent has been calculated in a planar superconductor-normal graphene-superconductor junction. Coupling between superconductor regions and graphene is taken into account by a tunneling Hamiltonian which contains two types of tunneling, intravalley and intervalley tunneling. Within the present tunneling approach, we find that the contributions of two kinds of tunneling to the critical supercurrent are completely separable. Therefore, it is possible to consider the effect of the intervalley tunnelings in the critical supercurrent. The incorporation of these type of processes into the tunneling Hamiltonian exposes a special feature of the graphene Josephson junctions. The effect of intervalley tunneling appears in the length dependence plot of critical current in the form of oscillations. We also present the results for temperature dependence of critical supercurrent and compare with experimental results and other theoretical calculations.

DOI: 10.1103/PhysRevB.85.024513 PACS number(s): 74.50.+r, 72.80.Vp

I. INTRODUCTION

In the past few years, after the first experimental synthesis by Geim *et al.*,[1] the community has witnessed the growing interest in monolayer carbon atoms arranged in a honeycomb lattice, called graphene. The peculiarity of graphene electronic structure is the primary reason which has given rise to such enthusiasm among scientists. Linear dispersion relation near the discrete Fermi points and chiral nature of carriers in graphene are responsible for the most intriguing phenomena that have been reported.[2,3]

Among the attractive properties of graphene, from both basic and applied points of view, are the superconductor proximity effect which has been studied experimentally and theoretically. Before any experimental observation, Beenakker[4] predicted in a seminal work that at the graphene-superconductor interface, not only the conventional Andreev retroreflection takes place, but also it can exhibit specular Andreev reflection owing to presence of two different valleys in the graphene band structure. Specular Andreev reflection takes place when an electron in the conduction band converts into a hole in the valance band. At the low doping level, specular reflections are dominated and at Dirac point all reflections are of this type.[5] By solving the Dirac–Bogoliubov–de Gennes (DBdGD) equations for an "ideal" normal-superconductor (NS) interface, in the short junction limit, in which the coherence length $\xi = \hbar v_F/\Delta_0$ (v_F is the Fermi velocity and Δ_0 the superconductivity order parameter) is much larger than junction length L, and with neglecting intervalley scatterings, Titov and Beenakker[6] and simultaneously Moghaddam and Zareyan[7] calculated the Andreev bound states, with which they obtained the Josephson supercurrent. Their results predicted the existence of a finite current even at the Dirac point. In these papers, to solve the DBdG equations, the rigid boundary condition was assumed, according to which the superconductivity gap has a fixed and finite value in the superconductor regions and it is zero in the normal region.

The first experimental investigation of the superconductor-graphene-superconductor (SGS) Josephson junction[8] showed that the Josephson current does flow through these junctions. This current depends strongly on the position of the Fermi energy and, as it had been predicted, there was a nonzero supercurrent at the neutral Dirac point. Afterward, several experimental studies have been conducted.[9–13] Recently, in addition to the critical supercurrent, direct measurement of the current-phase relation (CPR) has been performed with the interferometry technique.[14,15] The results confirm the predicted nonsinusoidal CPR curves[6] and show that the deviation from the sinusoidal behavior increases linearly with critical current.

At the same time, more theoretical efforts were triggered.[15–22] A self-consistent solution of the tight-binding DBdG equation, at zero temperature[16,17] and a later generalization to finite temperature,[18] have provided results on the dependence of the Josephson supercurrent on length, temperature, doping level, phase difference, and pairing symmetries of the superconductivity order parameter. Another method based on Cooper-pair propagation over long distances for junctions with $L \gg W$ also reveals such dependencies in the graphene Josephson junctions.[19,20] Shifting the Fermi energy away from zero point results in an enhancement in the critical supercurrent due to finite density of states at the Fermi level for $\mu \neq 0$. Besides the enhancement, one can see oscillations in the diagrams of the critical supercurrent as a function of length.[19–21]

In this paper we will use the perturbative Green's function method in the framework of the path integral and tunneling Hamiltonian between superconductor and normal graphene regions to calculate the critical Josephson supercurrent. An s-wave superconductivity pairing will be assumed in the superconductor areas of the graphene honeycomb lattice. In contrast to previous papers, we do not neglect the intervalley processes, as such processes may become important in the presence of edges, or external potentials with sharp variations.[23] Among the other circumstances where intervalley scattering becomes important, one can mention the presence of Kekule textures[24] which may arise from the creation of instantons of opposite

 ©2012 American Physical Society

sign in two valleys.[25] We will incorporate both types of intervalley and intravalley tunneling processes into the Hamiltonian. We will discuss the temperature and length dependence of the critical supercurrent. The advantage of the present tunneling approach is that, within this approach, contributions of intervalley and intravalley processes to the total Josephson supercurrent can be totally separated. Therefore, the effect of the intervalley tunneling on the critical current can be isolated. The present formulation reveals a peculiar feature of the graphene Josephson junctions which is the result of incorporating the intervalley tunnelings. In the curve of critical supercurrent as a function of junction length, the effect of intervalley tunneling appears in the form of oscillations which are drastically different from oscillations due to a nonzero chemical potential.

The paper is organized as follows. First, we summarize the perturbative Green's function method[26] and rephrase it for the eight-component spinors needed in the present paper. We then apply the formulation to the problem of SGS junctions. We close the paper by a discussion on the results.

II. METHOD AND MODEL

In a Josephson junction between two superconductors, a dissipationless supercurrent flows from one superconductor to the other to provide a state with minimum energy.[27] The critical supercurrent is given by

$$I = \frac{2e}{\hbar}\frac{\partial F}{\partial \varphi} \equiv I_c \sin(\varphi), \tag{1}$$

where F is the free energy of the system, I_c indicates the critical supercurrent, and $\varphi = \varphi_R - \varphi_L$ is the phase difference between two superconductors. In the framework of the path integral, the partition function is given by

$$Z = e^{-\beta F} = \int D[\bar{\Psi}]D[\Psi]e^{-S(\bar{\Psi},\Psi)}, \tag{2}$$

in which S is the effective action of system that is a function of Grassmann variables Ψ and $\bar{\Psi}$. In the imaginary time formalism ($\tau = it$), the action will be given by

$$S = \sum_{\vec{k}} \int_0^\beta d\tau \{\bar{\Psi}(\vec{k},\tau)\partial_\tau \Psi(\vec{k},\tau) + H[\bar{\Psi}(\vec{k},\tau),\Psi(\vec{k},\tau)]\}. \tag{3}$$

Here, H is the full Hamiltonian of the system that takes the form

$$\hat{H} = \hat{H}_L + \hat{H}_R + \hat{H}_N + \hat{H}_T. \tag{4}$$

$\hat{H}_L, \hat{H}_R, \hat{H}_N$, and $\hat{H}_T$ are, respectively, the Hamiltonian of the left and right superconductors, and the normal region and tunneling between superconductors and normal regions. The form of these Hamiltonians can be quite general, so that formula (12) holds under very general circumstances. The particular form of these Hamiltonians suitable for our own problem are given in Eqs. (13)–(15). If we express the matrix form of the above Hamiltonian as the sum of two parts, $\hat{T}$ as the tunneling term and $\hat{g}_0^{-1}$ for the rest, then in the basis $\hat{\Psi}(\vec{k}) \equiv [\hat{\Psi}(\vec{k}_L), \hat{\Psi}(\vec{k}_N), \hat{\Psi}(\vec{k}_R)]$, it can be written in the compact matrix form as

$$\hat{H} = \sum_{\{\vec{k}\}} \hat{\Psi}^\dagger(\vec{k})\big[\hat{g}_0^{-1} + \hat{T}\big]\hat{\Psi}(\vec{k}), \tag{5}$$

where $\hat{g}_0^{-1}$ and $\hat{T}$ are given by the following matrix forms:

$$\hat{g}_0^{-1} = \begin{pmatrix} g_{0L}^{-1} & 0 & 0 \\ 0 & g_{0N}^{-1} & 0 \\ 0 & 0 & g_{0R}^{-1} \end{pmatrix}, \tag{6}$$

$$\hat{T} = \begin{pmatrix} 0 & T_{NL} & 0 \\ T_{NL}^* & 0 & T_{NR}^* \\ 0 & T_{NR} & 0 \end{pmatrix}. \tag{7}$$

Here, g_{0L}^{-1}, g_{0N}^{-1}, and g_{0R}^{-1} are, respectively, the inverse propagators for the left, normal, and right areas excluding the tunneling parts.

After a Fourier transform, the effective action becomes

$$S = \sum_{\vec{k},i\omega_n} \bar{\Psi}(\vec{k},i\omega_n)\big[-i\omega_n \mathbb{I} + \hat{g}_0^{-1} + \hat{T}\big]\Psi(\vec{k},i\omega_n), \tag{8}$$

where $\hbar\omega_n = \pi k_B T(2n+1)$ are the Matsubara frequencies. With definition,

$$-\hat{G}_0^{-1} = -i\omega_n \mathbb{I} + \hat{g}_0^{-1}, \tag{9}$$

and from Eq. (2) we have

$$e^{-\beta F} = \int D[\bar{\Psi}]D[\Psi]e^{-\sum_{\vec{k},i\omega_n} \bar{\Psi}(\vec{k},i\omega_n)[-\hat{G}_0^{-1}+\hat{T}]\Psi(\vec{k},i\omega_n)}. \tag{10}$$

This is a Gaussian integral, which can be performed to lead to the following equation for the free energy:

$$\begin{aligned} F &= -\frac{1}{\beta}\mathrm{Tr}\ln\big[-\hat{G}_0^{-1} + \hat{T}\big], \\ &= -\frac{1}{\beta}\mathrm{Tr}\big[\ln\big(-\hat{G}_0^{-1}\big) + \ln(1 - \hat{G}_0\hat{T})\big]. \end{aligned} \tag{11}$$

Here, Tr means a summation over all diagonal matrix elements and an integration over all momenta. Having expanded this expression in terms of the tunneling amplitude, it can be readily shown that the fourth-order term is the first nonzero and leading term that contributes to the Josephson supercurrent. Using Eq. (1) and the identity $\ln\det\hat{A} = \mathrm{Tr}\ln\hat{A}$, the final expression for the supercurrent is obtained as

$$\begin{aligned} I(\varphi) &= \frac{-2e}{\hbar}\frac{1}{4\beta}\frac{\partial}{\partial\varphi}\mathrm{Tr}(\hat{G}_0\hat{T})^4 \\ &= \frac{-2e}{\hbar\beta}\frac{\partial}{\partial\varphi}\mathrm{Tr}[\hat{G}_L\hat{T}_{NL}\hat{G}_N\hat{T}_{NR}^*\hat{G}_R\hat{T}_{NR}\hat{G}_N\hat{T}_{NL}^*]. \end{aligned} \tag{12}$$

This matrix product shows a Cooper-pair propagation between two superconductors and electron tunnelings through interfaces and, as mentioned above, is a general formula for obtaining the critical supercurrent. Now let us specialize this equation to the special case of SGS junctions of this paper. The geometry of the graphene Josephson junction that we consider in this paper is depicted in Fig. 1. In the normal graphene region, the low-energy electrons are governed by the relativistic Dirac Hamiltonian $H_N = v_F(\vec{k}_N \cdot \vec{\sigma}) \otimes \tau_0$,

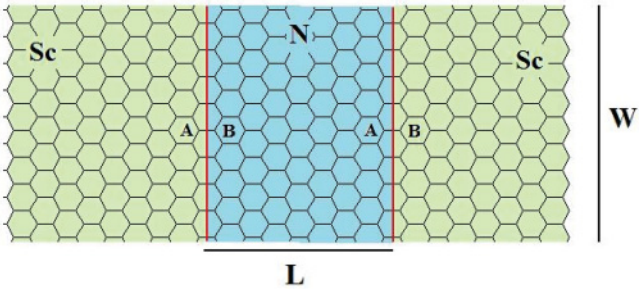

FIG. 1. (Color online) The schematic geometry of graphene Josephson junction. L is the separation of two superconductor (Sc) regions and W is the junction width.

where $v_F \simeq 10^6$ m/s is the Fermi velocity in graphene and $\vec{\sigma}$ and τ are Pauli matrices. $\vec{\sigma}$ operates on the sublattice degrees of freedom and τ_0 acts on the valley degree of freedom. Dirac fermions in graphene live in two different valleys, K and $\bar{K}$, on opposite corners of the Brillouin zone.

Pristine graphene cannot be a superconductor under ordinary conditions. Experimentally, to prepare a SGS junction, superconducting electrodes can be deposited on top of a graphene sheet, so that due to this proximity of superconductor electrodes to the graphene layer, the superconductivity order parameter can be assumed to be induced on the left and right graphene regions. Here, an s-wave superconductivity will be assumed in the left and right superconducting areas. In our model, the assumption is that the superconducting pairing takes place between two time-reversal electrons on the same sublattice but on different valleys in the Brillouin zone.[28] Thus the mean-field Hamiltonian for the superconducting part will be

$$\hat{H}^{\alpha}_{\mathrm{SC}} = \sum_{\vec{k},\sigma} \Delta_0 e^{i\varphi_\alpha} a^{\dagger}_{\vec{k},\sigma} \bar{a}^{\dagger}_{-\vec{k},-\sigma} + \Delta_0 e^{i\varphi_\alpha} b^{\dagger}_{\vec{k},\sigma} \bar{b}^{\dagger}_{-\vec{k},-\sigma} + \mathrm{H.c.}, \tag{13}$$

where a and b are fermion operators on sublattices A and B pertaining to valley K, while $\bar{a}$ and $\bar{b}$ denote the corresponding operators on valley $\bar{K}$. Δ_0 is the magnitude of the superconducting order parameter and φ_α denotes the phase of each $\alpha = R,L$ superconducting leads.

The electron tunneling between superconductors and the normal graphene region can be considered in several different ways. Here we have assumed one of the simplest models for electron tunneling in which the electrons tunnel through an atomically sharp interface. The independent contributions of the intervalley and the intravalley tunnelings to the critical supercurrent is a direct result of this simple model for tunneling Hamiltonian. As is depicted in Fig. 1, the superconductor and normal graphene are assumed to be connected to each other through their zigzag edge. The tunneling Hamiltonian contains left and right tunneling between the superconductor and normal graphene. As can be seen in Fig. 1, for the right side, electron tunneling takes place between sublattice A in the normal region and sublattice B in the superconductor region, while at the left interface, electrons tunnel between sublattice B in the normal region and sublattice A in the superconductor area. Therefore, the tunneling Hamiltonian in the tight-binding approximation can be written as

$$\hat{H}_T = \gamma_T \sum_i \hat{B}^{\dagger}_{iR} \hat{A}_{iN} + A^{\dagger}_{iL} \hat{B}_{iN} + \mathrm{H.c.}, \tag{14}$$

where γ_T is the tunneling amplitude and $\hat{A}$ and $\hat{B}$ generally stand for the Dirac fermion operators on the A and B sublattices and the summation extends over all atomic sites along the interfaces. By writing the Dirac fermion operators as the sum of two valley operators, the tunneling Hamiltonian for the right side will be given by

$$H^R_T = \gamma_T \sum_{k_N,k_R} e^{-i(k_{Nx}-k_{Rx})x_R} \big(b^{\dagger}_{k_R} a_{k_N} + e^{i\vec{Q}\cdot\vec{R}_R} \bar{b}^{\dagger}_{k_R} a_{k_N} + e^{-i\vec{Q}\cdot\vec{R}_R} b^{\dagger}_{k_R} \bar{a}_{k_N} + \bar{b}^{\dagger}_{k_R} \bar{a}_{k_N} \big) + \mathrm{H.c.}, \tag{15}$$

and likewise for the left interface. As can be seen, the tunneling Hamiltonian contains two types of tunneling, intravalley (first and last terms) and intervalley (second and third terms) tunnelings. Intervalley tunneling involves a "momentum transfer" $\vec{Q}$ that connects the two independent valleys in the Brillouin zone. Here because of the simple model in Eq. (14), both types of tunnelings occur with the same amplitude γ_T, however, in general they can take place with a different probability.

Now, let us define an appropriate basis to rewrite all parts of the Hamiltonian. A suitable representation for the Fermi operators is the following:

$$\Psi(\vec{k}) = (a^{\dagger}_{k\uparrow}, b^{\dagger}_{k\uparrow}, \bar{a}_{-k\downarrow}, \bar{b}_{-k\downarrow}, \bar{a}^{\dagger}_{k\uparrow}, \bar{b}^{\dagger}_{k\uparrow}, a_{-k\downarrow}, b_{-k\downarrow})^T. \tag{16}$$

In this basis, $\hat{G}^{-1}_{0N}$ and $\hat{G}^{-1}_{0\alpha}$ $(\alpha = R,L)$ are the block diagonal and one can easily obtain the required matrices by just inverting the blocks. The Green's function of the normal region is written as

$$\hat{G}^{-1}_{0N} = i\omega_n \mathbb{I} + \hbar v_F \begin{pmatrix} \vec{\sigma}\cdot\vec{k}_{N\uparrow} & 0 & 0 & 0 \\ 0 & \vec{\sigma}\cdot\vec{k}_{N\downarrow} & 0 & 0 \\ 0 & 0 & \vec{\sigma}^*\cdot\vec{k}_{N\uparrow} & 0 \\ 0 & 0 & 0 & \vec{\sigma}^*\cdot\vec{k}_{N\downarrow} \end{pmatrix}. \tag{17}$$

It is important to mention that in the normal area two electrons propagate between two superconductors as a Cooper pair with different spin. Thus, $\vec{k}_{N\uparrow}$ and $\vec{k}_{N\downarrow}$ are independent degrees of freedom in this region. For the superconductor Green's function we have

$$\hat{G}^{-1}_{0\alpha} = i\omega_n \mathbb{I}_{8\times 8} + [\mathbb{I}_{2\times 2} \otimes (\Delta_0 e^{i\varphi_\alpha \sigma_z} \sigma_x)] \otimes \mathbb{I}_{2\times 2} + \begin{pmatrix} -(\hbar v_F \vec{\sigma}\cdot\vec{k}_\alpha)\otimes\sigma_z & 0 \\ 0 & (\hbar v_F \vec{\sigma}^*\cdot\vec{k}_\alpha)\otimes\sigma_z \end{pmatrix}. \tag{18}$$

Finally, for the tunneling part of the Hamiltonian we have

$$T_{N\alpha} = \left[(e^{i\theta_\alpha \sigma_z}\sigma_x + \mathbb{I}_{2\times 2}) \otimes \begin{pmatrix} \delta^{\uparrow}_\alpha & 0 \\ 0 & -\delta^{\downarrow}_\alpha \end{pmatrix} \right] \otimes \mathbb{I}_\alpha, \tag{19}$$

where we use these notations:

$$\mathbb{I}_L = \frac{1}{2}(\sigma_x + i\sigma_y) = \begin{pmatrix} 0 & 1 \\ 0 & 0 \end{pmatrix}, \tag{20}$$

$$\mathbb{I}_R = \frac{1}{2}(\sigma_x - i\sigma_y) = \begin{pmatrix} 0 & 0 \\ 1 & 0 \end{pmatrix}, \tag{21}$$

$$\delta_\alpha^\sigma = \gamma_T e^{i(k_{Nx}^\sigma - k_{\alpha x})x_\alpha}, \quad e^{i\theta_\alpha} = e^{i\vec{Q}\cdot\vec{R}_\alpha}. \tag{22}$$

Now, we have all of the matrices needed for calculation of the free energy. From Eq. (12) and by using these matrices, we obtain

$$F = -\frac{16\Delta^2\gamma_T^4(\hbar v_F)^2}{\beta}\sum_{i\omega_n,\vec{k}}\frac{[(1+\cos\theta)k_x^\downarrow k_x^\uparrow + (-1+\cos\theta)k_y^\downarrow k_y^\uparrow - \sin\theta(k_x^\downarrow k_y^\uparrow + k_x^\uparrow k_y^\downarrow)]E_L^2E_R^2\cos[\varphi + (k_x^\downarrow - k_x^\uparrow)L]}{D_LD_R[(\hbar\omega_n)^2 + (\hbar v_F)^2k_\downarrow^2][(\hbar\omega_n)^2 + (\hbar v_F)^2k_\uparrow^2]}, \tag{23}$$

where $\vec{k}$ is a collective index denoting all possible momenta, i.e., $\vec{k} = \{\vec{k}_L, \vec{k}_R, \vec{k}_N^\uparrow, \vec{k}_N^\downarrow\}$. In Eq. (23), we have used the following notations:

$$\begin{aligned} \theta &= \theta_L - \theta_R = \vec{Q}\cdot\vec{L}, \\ D_\alpha &= (\hbar\omega_n)^4 + (\hbar v_F)^4k_\alpha^4 + \Delta_0^4 \\ &\quad + 2\big[(\hbar\omega_n)^2k_\alpha^2 + (\hbar\omega_n)^2\Delta_0^2 + \Delta_0^2k_\alpha^2\big], \\ E_\alpha^2 &= (\hbar\omega_n)^2 + \Delta_0^2 + (\hbar v_F)^2k_\alpha^2. \end{aligned} \tag{24}$$

The summation in Eq. (23) is over all Matsubara frequencies and all momenta around the pertinent valleys. In the limit of the wide junction limit, i.e., $W \gg L$, the details of the interface become irrelevant and we can replace the summation with an integration around the corresponding valley, up to an energy cutoff that the linear dispersion holds.

Due to symmetry of the integration region, even terms of the integrand can contribute to the free energy. With definition (1) for the critical supercurrent and from Eq. (23) we obtain (see the Appendix)

$$\begin{aligned} I_c = &\frac{128ek_BT\Delta^2(T)\gamma_T^4S^2(1+\cos\vec{Q}\cdot\vec{L})}{\hbar\pi^2} \\ &\times\sum_{\omega_n}[f(i\omega_n)g(i\omega_n)]^2, \end{aligned} \tag{25}$$

where $S = WL$ is the area of the junction and functions f and g are given by

$$f(i\omega_n) = \frac{1}{(\hbar v_F)^2}\int_0^{E_c}\frac{x\big[(\hbar\omega)^2 + \Delta_0^2(T) + x^2\big]dx}{x^4 + 2\big[(\hbar\omega_n)^2 + \Delta_0^2(T)\big]x^2 + (\hbar\omega_n)^4 + \Delta_0^4(T) + 2\Delta_0^2(T)(\hbar\omega_n)^2}, \tag{26}$$

$$g(i\omega_n) = \frac{1}{(\hbar v_F)^2}\int_0^{E_c}\frac{x\sin(x)dx}{\sqrt{x^2 + (\hbar\omega_n)^2}}\tan^{-1}\sqrt{\frac{1-x^2}{x^2 + (\hbar\omega_n)^2}}. \tag{27}$$

E_c is the cutoff energy and $\vec{L}$ indicates the vector connecting two superconducting leads.

Carefully tracing the above derivation shows that in Eq. (25) all effects of the intervalley tunneling processes appears in a term proportional to $\cos(\vec{Q}\cdot\vec{L})$. The elimination of the term proportional to $\sin(\vec{Q}\cdot\vec{L})$ can be physically understood: In view of symmetry of the problem under the $y \to -y$ transformation, the Hamiltonian is symmetric under $k_y \to -k_y$, which implies that the free energy must be symmetric with respect to the $\vec{Q} \to -\vec{Q}$ transformation. Hence only the term proportional to $\cos(\vec{Q}\cdot\vec{L})$ will survive in the free energy. Therefore, an oscillatory behavior in the critical supercurrent is predicted which is solely due to intervalley processes. It can be seen in the final result by setting $\vec{Q} = 0$, which amounts to ignoring the intervalley processes $[1 + \cos(\vec{Q}\cdot\vec{L})] \to g_v = 2$. This is the simple valley degeneracy expected in all extensive quantities, when the intervalley processes are ignored.[23]

The fact that the contribution of intervalley processes (both in tunneling and superconducting pairing) gives rise to an additive modulation by a wave vector $\vec{Q}$ is a feature of the present tunneling formulation. This shows that within the present formulation the contributions of two types of tunneling to the critical supercurrent are naturally separable, and reproduces to the proper degeneracy factor $g_v = 2$ in the limit where intervalley processes are ignored. As long as we have additive terms for intervalley and intravalley tunnelings in Eq. (15), there will be these two separable terms in the critical supercurrent. The oscillatory factors of $1 + \cos(\vec{Q}\cdot\vec{r})$ arise in other contexts, which require a convolution of Green's functions related to Dirac cones.[29] Also, as mentioned before, the two kinds of tunneling can take place with different amplitudes, but this cannot ruin the additive independent terms for contributions of these kinds of tunneling to the critical supercurrent. If this is the case, each term comes with its own amplitude in Eq. (25).

III. RESULTS AND DISCUSSION

To calculate the critical supercurrent from Eq. (25) we need to have the temperature dependence of the magnitude of superconductivity order parameter $\Delta(T)$. For s-wave superconductors the pair potential satisfies[30]

$$\ln\frac{\Delta(T=0)}{\Delta(T)}=2\sum_{n=1}^{\infty}(-1)^{n+1}K_0\left(\frac{n\Delta(T)}{k_BT}\right), \qquad (28)$$

where K_0 is the modified Bessel function and $\Delta_0(T=0)$ is the magnitude of the superconductivity gap at zero temperature. An analytical calculation of Eq. (25) is not feasible, thus we will calculate it numerically. The electron dispersion relation in graphene remains linear below a momentum cutoff that corresponds to $E_c=\hbar v_F k_c\approx 1$ eV. Careful scrutiny of Eq. (27) reveals an ω_n^{-6} dependence of the summand, so that it would rapidly decay at larger Matsubara frequencies. Therefore, it is adequate to sum over only the first few frequencies. We are now ready to present the results of calculations of the critical current using Eq. (25). As indicated before, we are in the wide junction limit ($W\gg L$), but we have no restriction on the distance between the superconductors, i.e., we can calculate the critical current for all range of the distances ($L<\xi$, $L\simeq\xi$, and $L>\xi$). Based on some experimental data from Ref. 15, we have assumed $\Delta_0(T=0)\simeq 6$ meV, which gives the superconductivity coherence length of the order of 10^2 nm. In all of our calculations we set $W=10\ \mu\text{m}\gg\xi$.

Figure 2 shows the length dependence of the critical current. The temperature at which the calculation has been performed is $0.1T_c$. In this figure, the curve with sharp oscillations shows the total critical current, while the smooth diagram gives the contribution of the intravalley tunneling processes to the critical current. As it is obviously expected, the current decreases by increasing the distance between two superconductors. The wavelength of the oscillations in this diagram $(1/Q)$ is of the order of a few angstroms. Therefore, we expect to see hundreds of oscillations within one coherence length. To clearly observe these oscillations, in the inset we have zoomed in a small distance on the length axis and have plotted the numerical results of Eq. (25) in this small length interval. In fact, the distinguishing feature of the intervalley electron tunneling is the oscillation with a characteristic wave vector $|\vec{Q}|$ in the total current. This suggests that if one measures the critical current versus the junction length, an oscillatory behavior is expected which can be attributed to the intervalley tunnelings.

The presence of a second valley connected to the first one by time-reversal symmetry is the reason for emergence of a specular Andreev reflection.[4,5] The present tunneling formulation reveals that the existence of two valleys leads to another peculiar feature in the Josephson current through graphene, namely, oscillatory behavior of the Josephson current as a function of the junction length L. In fact, our results in Fig. 2 shows that, for some distance between two superconducting electrodes, the critical supercurrent will be strongly suppressed due to intervalley tunnelings between the normal and superconducting regions. This can be physically interpreted as the destructive interference between the supercurrent arising from Andreev bound states,[7] and those arising from Andreev modes[4] (made possible by specular reflections).

In fact, dropping of the normal region enhances the critical supercurrent and leads to the emergence of oscillations in the diagram of the critical current,[17] regardless of the Fermi-wave-vector mismatch between the normal and superconductor regions. Note that, in all our calculations, an undoped normal graphene region has been assumed, so that undoubtedly the doping[19–21] is not responsible for the oscillatory behavior of the critical supercurrent. Figure 2 clearly shows that only the intervalley tunneling processes are responsible for such oscillations.

One should note that taking an atomically sharp interface model in Eq. (14) has resulted in such a crucial oscillatory term $\cos(\vec{Q}\cdot\vec{L})$ in the final expression for critical supercurrent. But in the real samples, such sharp interfaces can hardly be realized and in most of the time we have rough interfaces. In these cases,

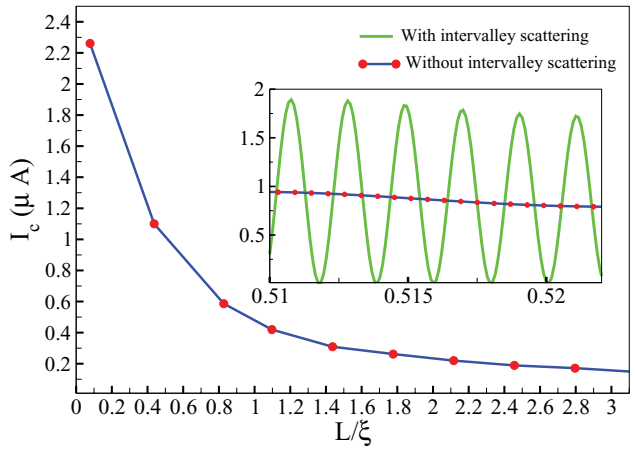

FIG. 2. (Color online) Plot of the critical supercurrent as a function of junction length for $T=0.1\,T_c$. The green (light gray) line with sharp oscillations in the inset shows the total critical current and the blue (dark gray) line presents the contribution of the intravalley tunneling processes to the critical supercurrent.

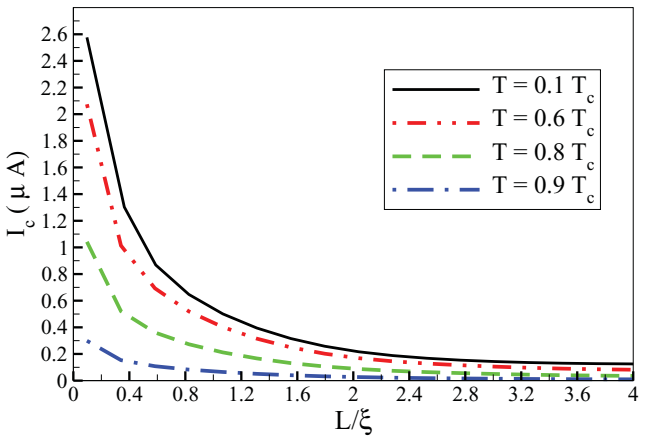

FIG. 3. (Color online) The critical supercurrent as a function of junction length for different temperatures. For easier comparison, in this plot, the intervalley tunneling processes have not been taken into account. Decreasing the critical supercurrent by increasing the junction length and temperature is clearly seen in these curves.

the oscillatory term could be averaged and sharp oscillations in the diagram will be smoothed.

Figure 3 presents the length dependence of the critical supercurrent for different temperatures. In this plot, to show the general dependence of the critical current on the junction length more clearly, and also to facilitate comparison with other papers which do not consider intervalley tunneling, we have only retained the intravalley tunnelings. It is clearly seen that the critical supercurrent suddenly decreases in all diagrams, when one approaches $L \approx \xi$ from below. Furthermore, regarding the temperature dependence, it drops very rapidly when temperature approaches the critical temperature. Our results are in a good agreement with the results of the self-consistent tight-binding method [Fig. 5(a) in Ref. 16 and Fig. 11(a) in Ref. 17].

In Fig. 4, we have plotted the contribution of the intravalley processes to the critical supercurrent as a function of temperature. The results are displayed separately for distances below the coherence length, $L < \xi$ (up panel), and distances above it, $L > \xi$ (down panel). The up panel of this figure agrees with results of Ref. 20. When one compares the temperature dependence for junction lengths less than the coherence length, with those above the coherence length, a clear qualitative difference can be observed: For distances below the coherence length, there is a plateau in supercurrent for temperatures smaller than 0.5 T_c and after that all diagrams reach zero near to $T = T_c$. But for distances above the coherence length, after a much shorter plateau, an exponential decay takes place for temperatures near T_c. As one can see in Fig. 4, the temperature at which a rapid decrease sets in decreases by increasing the junction length.

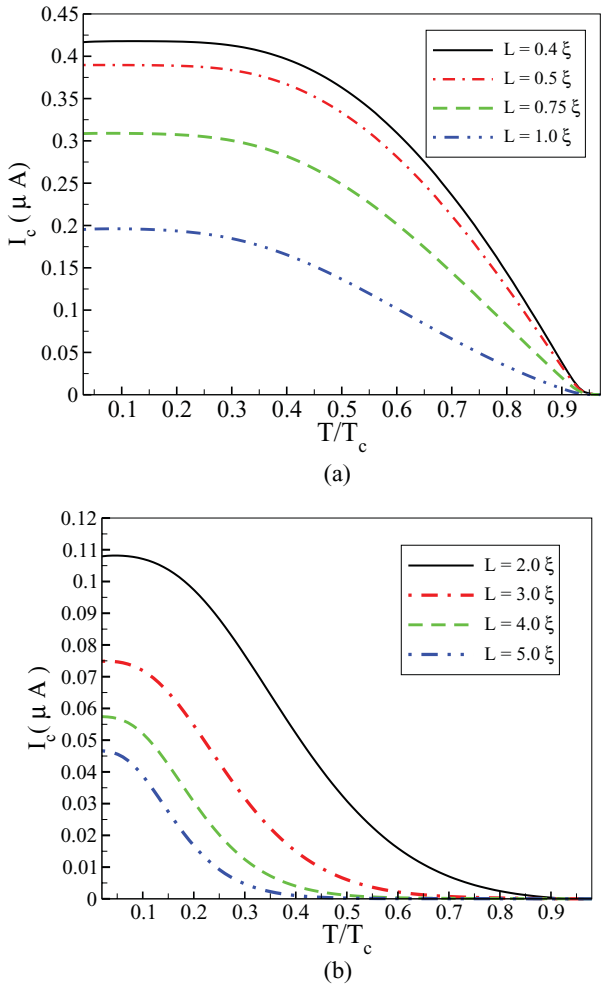

FIG. 4. (Color online) Temperature dependence of the critical supercurrent for different junction lengths (up) for $L < \xi$ and (down) $L > \xi$. Notice that in these diagrams only the contribution of the intravalley tunnelings to the critical current, have been taken into account.

The temperature dependence of the critical current has been measured in several research papers. Our results are qualitatively consistent with these experimental measurements. In particular, when a comparison between the observations in Refs. 11 and 13 is made, the above-mentioned different behaviors of temperature dependence of the critical current can be noticed. Therefore, from our calculations, we judge that in samples of Ref. 11 the junction length is smaller than the coherence length, while for those in Ref. 13 the length of the junctions seems to be above the coherence length. Similar temperature dependencies have been obtained in the other theoretical papers. For example, in Fig. 2 of Ref. 18 and Fig. 3 of Ref. 20, for $L < \xi$ and $L > \xi$, similar results have been obtained. Finally, in Fig. 5 the total critical supercurrent as a function of temperature has been plotted. In this diagram both intervalley and intravalley tunnelings have been taken into account. As can be seen in this figure, the variation of critical current with the junction length is different from diagrams of Fig. 4, which is a consequence of the oscillatory behavior of the critical current as a function of the junction length. Otherwise, the general trends are similar to those in Fig. 4.

In summary, we employed a method based on the perturbative Green's function in the framework of the path integral to calculate the critical supercurrent in the graphene Josephson junction. Our results presented the length and temperature dependence of the critical supercurrent. The role of the intervalley tunnelings in the supercurrent has been investigated, and it is shown that incorporating these kind of tunnelings led to sharp oscillations in the behavior of critical current as a function of the junction length. Comparison of our results with

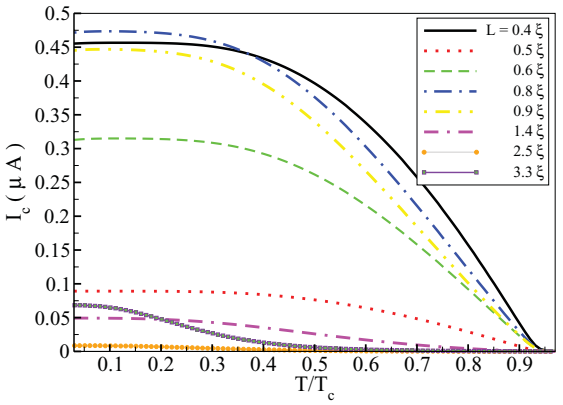

FIG. 5. (Color online) Plot of the total critical supercurrent as a function of temperature for different values of the distance between superconducting electrodes. In contrast to the diagrams of Fig. 4, in this diagram the contributions of all processes have been calculated.

the results that have been obtained by the other formalisms, and also with experimental observations, suggests that the junctions realized in experiment are likely to be in the weak tunneling regime, which are consistent with perturbative treatment.

ACKNOWLEDGMENTS

We thank F. Shahbazi and A. Vaezi for insightful comments and discussions. S.A.J. was supported by the National Elite Foundation (NEF) of Iran. We thank an anonymous referee for very useful comments.

APPENDIX: DETAILS OF CALCULATIONS

To obtain Eq. (25) from Eq. (23), we should expand the numerator of Eq. (23). For convenience, we replace $k_x^{\downarrow}L$, $k_x^{\uparrow}L$, $k_y^{\downarrow}L$, and $k_y^{\uparrow}L$, respectively, with x, x', y, and y'. There are two main terms: For the one proportional to $\sin\varphi$, we have

$$\sin\varphi\{[(1+\cos\theta)xx'+(-1+\cos\theta)yy'-\sin\theta(xy'+x'y)] \times[\sin x\cos x'-\cos x\sin x']\}. \tag{A1}$$

These terms are odd functions at least with respect to one of their variables, while the integration region is even respect to all variables, and hence they do not have contribution to the free energy. The other term is proportional to $\cos\varphi$,

$$\cos\varphi\{[(1+\cos\theta)xx'+(-1+\cos\theta)yy'-\sin\theta(xy'+x'y)] \times[\cos x\cos x'+\sin x\sin x']\}. \tag{A2}$$

After careful consideration we find out that only the term proportional to $xx'\sin x\sin x'$ has a nonzero contribution to the free energy. Therefore, the remaining integration corresponding to normal region variables is of this type:

$$\int_{-E_c}^{E_c}dy\int_{-\sqrt{E_c^2-y^2}}^{\sqrt{E_c^2-y^2}}dx\,\frac{x\sin x}{(\hbar\omega_n)^2+x^2+y^2}. \tag{A3}$$

Integration of variable y can be performed analytically, which gives

$$2\int_0^{E_c}dx\,\frac{x\sin x}{\sqrt{(\hbar\omega_n)^2+x^2}}\arctan\sqrt{\frac{E_c^2-x^2}{(\hbar\omega_n)^2+x^2}}. \tag{A4}$$

[1] K. S. Novoselov, A. K. Geim, S. V. Morozov, D. Jiang, Y. Zhang, S. V. Dubonos, I. V. Grigorieva, and A. A. Firsov, Science **306**, 666 (2004).
[2] A. K. Geim and K. S. Novoselov, Nat. Mater. **6**, 183 (2007).
[3] A. H. Castro Neto, F. Guinea, N. M. R. Peres, K. S. Novoselov, and A. K. Geim, Rev. Mod. Phys. **81**, 109 (2009).
[4] C. W. J. Beenakker, Phys. Rev. Lett. **97**, 067007 (2006).
[5] C. W. J. Beenakker, Rev. Mod. Phys. **80**, 1337 (2008).
[6] M. Titov and C. W. J. Beenakker, Phys. Rev. B **74**, 041401 (2006).
[7] A. G. Moghaddam and M. Zareyan, Phys. Rev. B **74**, 241403 (2006).
[8] H. B. Heersche, P. Jarillo-Herrero, J. B. Oostinga, L. M. K. Vandersypen, and A. F. Morpurgo, Nature (London) **446**, 56 (2007).
[9] H. B. Heersche, P. Jarillo-Herrero, J. B. Oostinga, L. M. K. Vandersypen, and A. F. Morpurgo, Eur. Phys. J. Special Topics **148**, 27 (2007).
[10] A. Shailos, W. Nativel, A. Kasumov, C. Collet, M. Ferrier, S. Guéron, R. Deblock, and H. Bouchiat, Europhys. Lett. **79**, 57008 (2007).
[11] X. Du, I. Skachko, and E. Y. Andrei, Phys. Rev. B **77**, 184507 (2008).
[12] C. M. Ojeda-Aristizabal, M. Ferrier, S. Gueron, and H. Bouchiat, Phys. Rev. B **79**, 165436 (2009).
[13] D. Jeong, J. H. Choi, G. H. Lee, S. Jo, Y. J. Doh, and H. J. Lee, Phys. Rev. B **83**, 094503 (2011).
[14] C. Girit, V. Bouchiat, O. Naaman, Y. Zhang, M. F. Crommie, A. Zettl, and I. Siddiqi, Phys. Status Solidi B **246**, 2568 (2009).
[15] C. Chialvo, I. C. Moraru, D. J. Van Harlingen, and N. Mason, e-print arXiv:1005.2630.
[16] A. M. Black-Schaffer and S. Doniach, Phys. Rev. B **78**, 024504 (2008).
[17] J. Linder, A. M. Black-Schaffer, T. Yokoyama, S. Doniach, and A. Sudbo, Phys. Rev. B **80**, 094522 (2009).
[18] A. M. Black-Schaffer and J. Linder, Phys. Rev. B **82**, 184522 (2010).
[19] J. Gonzalez and E. Perfetto, Phys. Rev. B **76**, 155404 (2007).
[20] J. Gonzalez and E. Perfetto, J. Phys. Condens. Matter **20**, 145218 (2008).
[21] I. Hagymasi, A. Kormanyos, and J. Cserti, Phys. Rev. B **82**, 134516 (2010).
[22] Q. Sun and X. C. Xie, J. Phys. Condens. Matter **21**, 344204 (2009).
[23] S. Das Sarma, S. Adam, E. Hwang, and E. Rossi, Rev. Mod. Phys. **83**, 407 (2011).
[24] Chang-Yu Hou, C. Chamon, and C. Mudry, Phys. Rev. Lett. **98**, 186809 (2007).
[25] A. Vaezi and Xia-Gang Wen, e-print arXiv:1101.1662.
[26] M. Mori, S. Hikino, S. Takahashi, and S. Maekawa, J. Phys. Soc. Jpn. **76**, 054705 (2007).
[27] B. D. Josephson, Phys. Lett. **1**, 251 (1962)
[28] N. B. Kopnin and E. B. Sonin, Phys. Rev. B **82**, 014516 (2010).
[29] S. Saremi, Phys. Rev. B **76**, 184430 (2007); M. Sherafati and S. Satpathy, *ibid.* **83**, 165425 (2011).
[30] A. A. Abrikosov, L. P. Gorkov, and I. Y. Dzyaloshinskii, *Quantum Field Theoretical Methods in Statistical Physics*, 2nd ed. (Pergamon, Oxford, UK, 1965).